

Methods of Computer Simulation - Project Report

Candidate Number: 1090111

April 2025

QUESTION 1

The quantity

$$\Delta E = \frac{1}{N_{step}} \sum_{i=1}^{N_{step}} \left| \frac{E_i - E_0}{E_0} \right|$$

where E_0 is the initial total energy and E_i that for the i^{th} time step, provides a measure of energy conservation in a molecular dynamics trajectory.

For a 1-dimensional harmonic oscillator, comparing molecular dynamic runs of equal total time, compute ΔE as a function of the time step δt for the Velocity-Verlet integrator. Show your results on a log-log plot. Comment on the scaling you observe.

The Velocity-Verlet Algorithm applied to a Molecular Dynamics simulation is characterised by the following steps:

1. Give atom(s) initial positions
2. Compute the forces acting on the atom(s) and choose a δt :

$$F = ma = -kx \quad (1)$$

$$a = \frac{F}{m} = \frac{-kx}{m} \quad (2)$$

3. Move atom(s) according to the Velocity-Verlet algorithm:

$$x_{i+1} = x_i + v_i \delta t + \frac{1}{2} a_i (\delta t)^2 \quad (3)$$

4. Move time forward by $t + \delta t$
5. Repeat over a chosen time period

In this simulation, the system was evolved over five time periods, each of duration 2π , to reflect the sinusoidal nature of the harmonic oscillator. A more physically representative total time allows for more accurate assessment of long-term energy conservation. Time steps δt were spaced logarithmically from 10^{-3} to 10^0 . The simulation was conducted in atomic units to simplify the dynamics and to reduce dimensional complexity.

After running the simulation, the average energy deviation ΔE was plotted against the time step δt on a log-log scale, as shown in Figure 1.

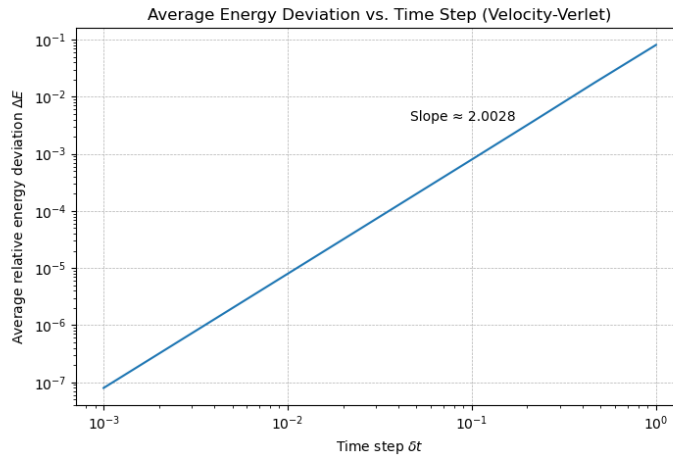


Figure 1: Average Energy Deviation as a function of time step

As shown in Figure 1, the error in the energy calculations increases with the time step δt . For small time steps (e.g. $\delta t = 10^{-3}$), the deviation is minimal. As δt increases, the number of integration steps decreases, resulting in less accurate simulations.

A linear fit on the log-log scale yields a slope of approximately 2.0028, indicating that the energy error scales as $(\delta t)^2$. This is consistent with the Velocity-Verlet algorithm being second-order accurate in time.

To further demonstrate that the energy is indeed conserved throughout this simulation, additional plots were generated for $\delta t = 0.001$. These plots can be found in Figure 2.

The first plot shows the total energy as a function of time, with a dashed line indicating $E(0)$.

The energy remains nearly constant, with only very small oscillations around the initial value. A phase-space diagram of velocity versus position also confirms the conservation of energy, with the trajectory forming a near-perfect circle centred at the origin. This is characteristic of an ideal harmonic oscillator. Zoomed-in views of the energy deviation $E(t) - E(0)$ are provided in two subplots with different vertical scales to illustrate the extremely small deviations from zero.

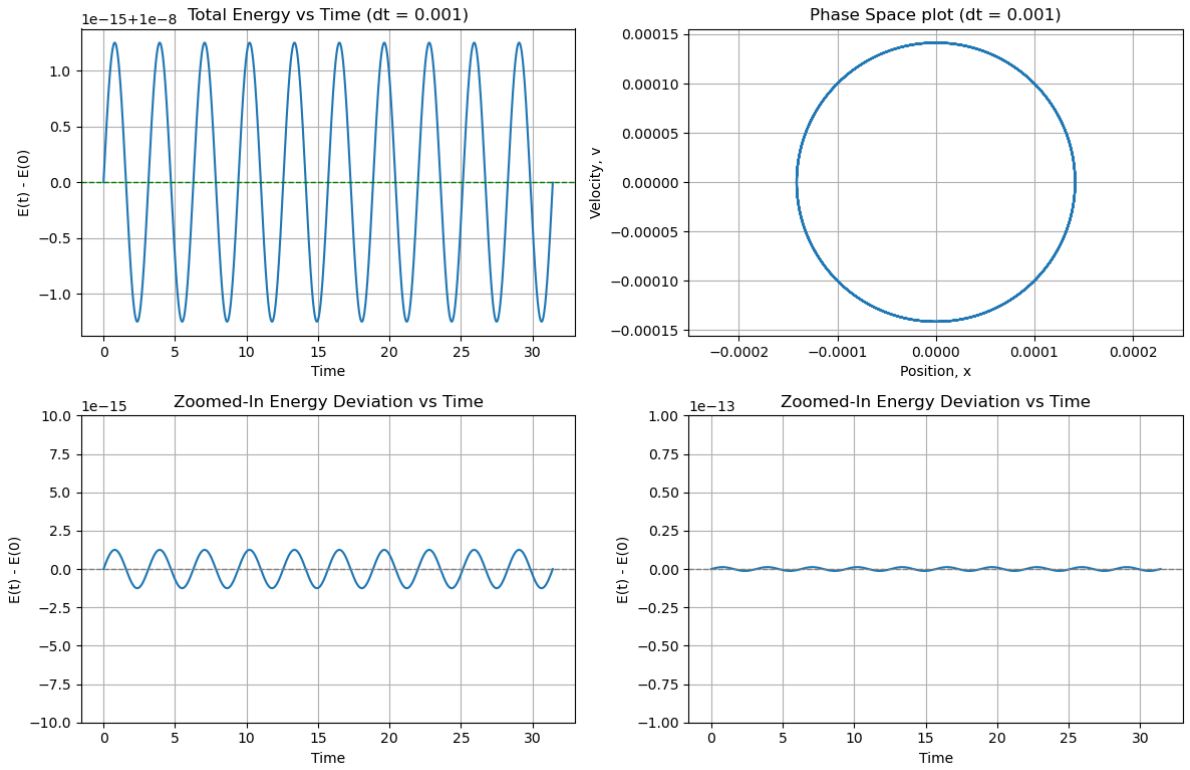


Figure 2: Various plots showing energy conservation for this simulation

QUESTION 2

Consider a system for which the energy is a function of only one variable (x) and is given by:

$$P(x) \propto \exp[-\beta E(x)] = \begin{cases} 1 & \text{if } 0 \leq x < 1 \\ 0 & \text{if } x < 0 \text{ or } x \geq 1 \end{cases}$$

We wish to use Monte Carlo to simulate this system, and consider two algorithms that differ in the types of moves used.

1. Add a random displacement between $[-\delta, \delta]$ to x .
2. Generate a random number ϕ between $[0, 1]$. With probability of 0.5 invert the value of ϕ . Scale x by ϕ .

By considering the generating probability distributions for the two move types, derive the correct acceptance criteria for both schemes.

What will happen if the acceptance criterion for (a) is used for (b)?

Part 1

For this question, the choice was made to not run the simulation over a uniform number of steps. Instead, the choice was made to include a number of equilibration steps to ensure that the system reaches equilibrium before data collection begins. The simulation was run for 10^7 steps, with the first half used for equilibration and the second half for data collection. δ was set at 0.1 to ensure a happy medium between accuracy and simplicity.

The Metropolis-Hastings algorithm, characterised by the steps below, was used.

1. Initialise
 - (a) Pick an initial state x_0
 - (b) Set $t = 0$
2. Iterate
 - (a) Generate a random candidate state x' according to $g(x'|x_t)$
 - (b) Calculate the acceptance probability
$$A(x', x) = \min \left(1, \frac{P(x')}{P(x)} \frac{g(x|x')}{g(x'|x)} \right) \quad (4)$$
3. Accept or reject:
 - (a) Generate a uniform random number $x \in [0, 1]$;
 - (b) If $x \leq A(x', x_t)$ then accept the new state and set $x_{t+1} = x'$
 - (c) If $x > A(x', x_t)$, then reject the new state and copy the old state forward, $x_{t+1} = x_t$
4. Set $t = t + 1$

Since the distribution is uniform between $[0, 1]$ and the displacement is symmetrical,

$$\frac{g(x|x')}{g(x'|x)} = 1$$

and the acceptance criterion for this problem is simply given by

$$A(x', x) = \min \left(1, \frac{P(x')}{P(x)} \right) \quad (5)$$

The symmetrical nature of adding the displacement means that any proposed state x' that falls within the uniform distribution $[0, 1]$ will be accepted.

Running the simulation for this acceptance criterion generates a histogram where the value of the accepted state is plotted against its frequency. This plot can be seen in Figure 3.

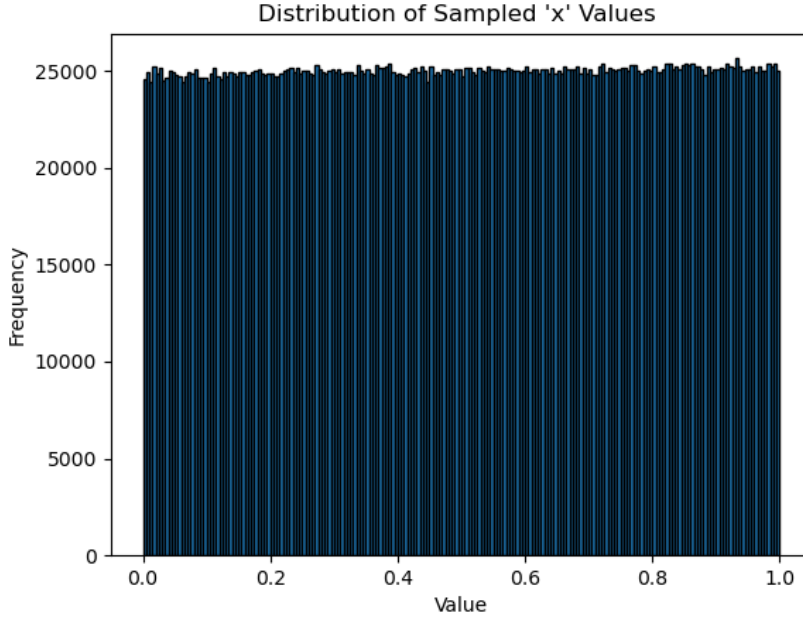


Figure 3: Histogram of accepted 'x' values and their acceptance frequency

Looking at Figure 3, it is clear that each value of x' occurs with nearly the same frequency. The acceptance rate for this simulation is approximately 95%. This high acceptance rate is expected, given the small value of $\delta = 0.1$, which limits proposals to small displacements that mostly remain within the allowed range. High acceptance rates are generally favoured, as they ensure that the simulation explores the full space efficiently. However, if moves are too small, exploration may be slow despite the high acceptance. This trade-off can be adjusted by tuning δ .

Part 2

Part two of the question uses the same Metropolis-Hastings algorithm as part one, albeit that the acceptance criterion will be different due to the asymmetry of the condition placed on this simulation. The acceptance criterion for this simulation must account for the asymmetry of the proposal distribution. In this case, the proposed move is a scaled version of the current $x' = \phi x$, where $\phi \in [1, 1 + \delta] \cup \left[\frac{1}{1 + \delta}, 1\right]$. Because this transformation is not symmetric, the Metropolis-Hastings criterion includes the ratio of the proposal densities:

$$A(x', x) = \min\left(1, \frac{P(x')}{P(x)} \cdot \frac{g(x|x')}{g(x'|x)}\right)$$

Due to the nature of the scaling move, the probability densities transform with a Jacobian determinant. This leads to the proposal ratio being:

$$\frac{g(x|x')}{g(x'|x)} = \frac{1}{\phi^2}$$

Thus, the correct acceptance criterion becomes:

$$A = \min\left(1, \frac{1}{\phi^2}\right)$$

Now, the working algorithm becomes:

1. Generate a random number in $[0, 1)$ and assign to x_0
2. If the randomly generated number $u < 0.5$, then sample $\phi \in [1, 1 + \delta]$
3. If the randomly generated number $u \geq 0.5$, then sample $\phi \in \left[\frac{1}{1+\delta}, 1\right]$
4. Assign $\phi \cdot x_0$ to the variable x' .
5. If $10^{-4} < x' < 1$, then:

$$A = \min\left(1.0, \frac{1.0}{(\phi)^2}\right)$$

- (a) If a randomly generated number $u < A$, then set $x_0 = x'$

The histogram generated by running the simulation for part 2 can be seen in Figure 4.

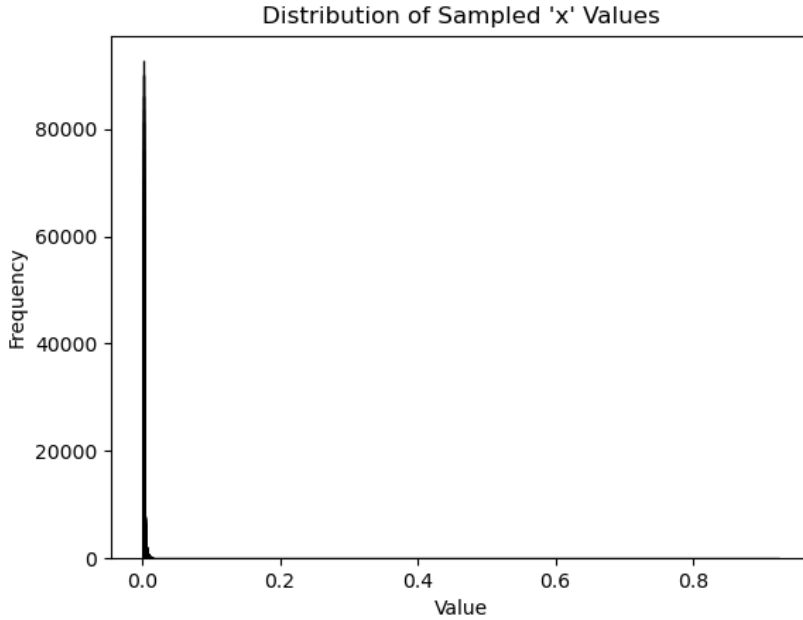


Figure 4: Part (b) Histogram of accepted 'x' values and their acceptance frequency

Looking at Figure 4, it is clear that the different accepted values of x' are no longer occurring at the same frequency as they did in part 1.

The accepted values of x' become increasingly concentrated near zero, due to the bias introduced by the asymmetric proposal combined with the Jacobian-corrected acceptance probability. The acceptance rate for this scheme is approximately 92.05%, which may seem high, but it arises because most proposals result in relatively small scalings (since $\delta = 0.1$). Despite the high acceptance, the sampled values cluster heavily near zero, indicating poor sampling of the full space. This highlights that a high acceptance rate alone does not guarantee good exploration.

The same simulation was repeated, but using the acceptance criterion from part 1 instead of the one derived for the asymmetric proposal. This means that step 1-4 from part 2 are still the same, but the acceptance criterion now becomes: If $0 \leq x' \leq 1 \rightarrow x_0 = x'$. The resulting histogram can be seen in Figure 5.

Changing the acceptance criterion has a significant influence on the resulting histogram. When the acceptance criterion from Part 1 is applied to the asymmetric proposal in Part 2, the balance is off. Nonetheless, the simulation achieves an acceptance rate of approximately 98.87%. This occurs because

nearly all proposed scalings fall within the allowed range, and no proper rejection mechanism based on asymmetry is in place. The resulting distribution is still skewed towards lower values of x , though less severely than when using the asymmetric criterion. However, it is important to note that removing the rejection bias is the reason for the change in skewing. The proposal bias remains, so the simulation is still being run wrong. This highlights the importance of using the correct acceptance rule, as using an inappropriate rule can yield misleading results even when acceptance rates appear favourable.

Ultimately, these different conditions show that the acceptance criteria are of great significance to the performance of the simulation. In part (a), δ controls the jump size. Therefore, for a small δ as per our case, most proposals will be accepted, but there is slower exploration of the sample size. In part (b), δ controls how much scaling is allowed. With a small δ , ϕ will get closer to 1. As a result, the simulation proceeds via small multiplicative updates. This gives a high acceptance rate but with poor space coverage. These results demonstrate that δ plays a crucial role in controlling both the acceptance rate and the sampling efficiency. While high acceptance rates (as seen here) are not inherently problematic, they may reflect overly conservative proposals that limit exploration. In practice, one aims to tune δ to balance acceptance and exploration, with typical target rates in the range of 20 – 40% when exploring complex energy systems ¹.

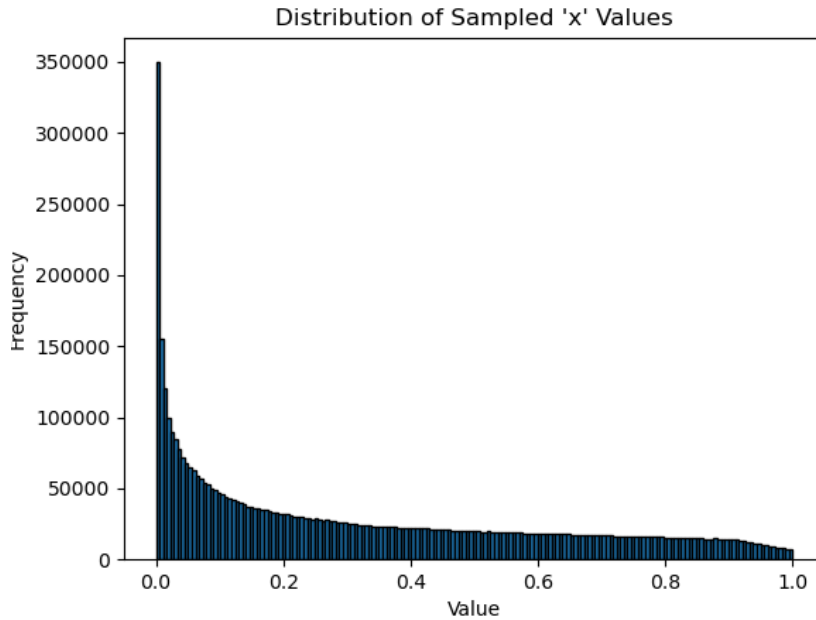


Figure 5: Part (c) Histogram of accepted 'x' values and their acceptance frequency

Summary Table of Simulation Results

The table below summarizes both the *acceptance rates* (a measure of the algorithm's efficiency) and the *average sampled values of x* (a measure of the equilibrium distribution each method produces).

Algorithm	Acceptance Rate (%)	Mean Sampled x
(a) Symmetric displacement	95.00	0.5013
(b) Correct scaling move	92.05	0.0029
(b) with criterion from (a)	98.87	0.3223

Table 1: Comparison of different Monte Carlo sampling schemes. The acceptance rate indicates the percentage of proposals accepted during the simulation. The average x value reflects the equilibrium distribution resulting from each algorithm.

¹Prokhorenko, S., Kalke, K., Nahas, Y. et al. *Large scale hybrid Monte Carlo simulations for structure and property prediction. npj Comput Mater*, 4, 80 (2018), Accessed: 17-04-2025

QUESTION 5

Write a Monte Carlo programme to simulate the 2D Ising model on a square lattice with nearest-neighbour ferromagnetic interactions. Use single spin flips as the basic Monte Carlo move.

Compute the heat temperature dependence of the magnitude of the magnetisation, heat capacity and magnetic susceptibility. Explore the dependence of the results on the system size and comment on the trend.

Estimate the transition temperature at zero field.

The 2D Ising model

In statistical mechanics, the 2D Ising model is often used to provide a microscopic description of ferromagnetic materials. Raising the temperature on a ferromagnetic material will increase movements within the atom and allow its magnetic moment to align its direction. This happens when the temperature of the ferromagnetic material is below the Curie (or critical) temperature T_c . Heating the ferromagnetic material over the Curie temperature allows the ferromagnetic material to randomly orient its spins, leading to the paramagnetic phase of the material. Thus, the Curie temperature can be viewed as a phase transition temperature ².

The 2D Ising model is therefore characterised by a square lattice of spins which are located on the sites of the lattice. These spins will only exhibit spins of ± 1 and will interact with their nearest neighbours on the lattice with coupling strength constant $J > 0$. Note that for the 2D Ising model, each spin on a lattice site has four nearest neighbours. The Hamiltonian, \mathcal{H} , for the 2D Ising model is thus given by ³

$$\mathcal{H} = -J \sum_{\langle i,j \rangle} S_i S_j - H \sum_i S_i \quad (6)$$

where $S_i = \pm 1$ denotes the spin at site i and H represents the external magnetic field.

To simplify the simulation, the Boltzmann constant k_B and coupling strength constant J are fixed at 1, while H is set to 0 to signify a zero field. The transition temperature T_c is given by

$$\tanh\left(\frac{2J}{k_B T}\right) = \frac{1}{\sqrt{2}} \quad (7)$$

and therefore, at $J = k_B = 1$,

$$T_c = \frac{2}{\ln(1 + \sqrt{2})} = 2.269185... \quad (8)$$

One must study various observables in order to determine a material's transition temperature.

The observables most commonly studied in the context of the 2D Ising model are the average magnetisation, $\langle |M| \rangle$, given by

$$\langle |M| \rangle = \left\langle \left| \frac{1}{N} \sum_i S_i \right| \right\rangle \quad (9)$$

the average energy, $\langle E \rangle$, given by

$$\langle E \rangle = \left\langle \frac{1}{N} \sum_{ij} -S_i S_j \right\rangle \quad (10)$$

the heat capacity, given by

$$C_t = \frac{\langle E^2 \rangle - \langle E \rangle^2}{NT^2} \quad (11)$$

and the magnetic susceptibility, \mathcal{X} , given by

$$\mathcal{X} = \frac{\langle M^2 \rangle - \langle M \rangle^2}{NT^2} \quad (12)$$

²L. Rohman *et al*, 2019, *J. Phys.: Conf. Ser.* **1170** 012018, Accessed: 17-04-2025

³M. Kim, *Measures for Complexity and the Two-dimensional Ising model*, 2011, p.5, Accessed: 17-04-2025

where S_i denotes the spin at site i , S_j denotes the spin at site j , N denotes the $L \times L$ square lattice and T denotes the temperature. Due to the inclusion of the constant N , all observables are calculated based on a normalisation per spin. A table with the simulation parameters for the different lattice sizes can be found in Table 2.

PARAMETER	L = 20	L = 40	L = 60
Lower temperature range	$T \in [1.5, 2.0]$ in 10 steps	same	same
Core temperature range	$T \in [2.0, 2.6]$ in 50 steps	same	same
Higher temperature range	$T \in [2.6, 3.5]$ in 10 steps	same	same
Number of MC steps	10000	20000	50000
Fraction of steps used for equilibration	0.25	0.25	0.3
Random seed	13–18	13–23	13–23
Number of independent runs	5	10	10

Table 2: Simulation parameters for different lattice sizes L

The Metropolis Monte Carlo algorithm for this simulation is given below.

1. Initialise

- (a) Build an $L \times L$ lattice of ± 1 spins
- (b) Set $N_{steps} = 0$

2. Iterate

- (a) Generate a random candidate lattice state
- (b) Determine the lattice energy (ΔE_j) for the lattice site
- (c) Calculate the acceptance probability

$$A(x', x) = \min \left(1, \frac{P(x')}{P(x)} \frac{g(x|x')}{g(x'|x)} \right) \quad (13)$$

3. Accept or reject:

- (a) If $\Delta E_j < 0$, accept spin-flip and update energy
 - (b) Generate a random number
 - i. If the randomly generated number $< \exp \left(\frac{-\Delta E_j}{T} \right)$, accept spin-flip and update energy
- Note that $\mathcal{P} \propto \exp \left(\frac{-\Delta E_j}{k_B T} \right) = \exp \left(\frac{-\Delta E_j}{T} \right)$ since $k_B = 1$

4. Set $N_{steps} = N_{steps} + 1$

Simulation Results

When working on this simulation, it was fairly obvious that the scale of this simulation had to be of at least order 10^4 in order to produce meaningful results. It was also noticed that increasing the lattice size introduced a noticeable amount of noise, especially at low temperature. Therefore, the decision was made to increase Monte Carlo steps for higher lattice sizes as well as expanding the equilibration phase to allow the noise to equilibrate properly. These decisions are reflected in the chosen parameters as presented in Table 2 above. However, increasing not only lattice sizes, but also Monte Carlo steps comes with a sharp increase in computational runtime. Thus, after investigation, the decision was made to use the NUMBA and multiprocessing packages in Python to drastically decrease runtime. As a result, a simulation that initially took $\sim 6h$ now only takes $\sim 1h$.

When it comes to investigating trends across the data, a separate Python script was written with the sole purpose of analysing and plotting the obtained data. This script first loads the data saved from the simulation before smoothing the functions. After smoothing, the data is plotted. This plot can be found in Figure 6.

It is clear that after smoothing, the data is no longer subject to extreme fluctuations due to noise. This is still present for the 'small' 20×20 lattice and is to be expected. In a relatively small lattice, any changes in spin have more significant consequences on its observables than for larger lattices. When working with larger lattices, it is expected that these fluctuations decrease, which is indeed reflected in the plots.

When working in the thermodynamic limit, spontaneous changes in symmetry cause a sharp discontinuity in magnetisation at T_C . For finite lattices, thermal fluctuations dominate instead and the magnetisation decreases smoothly, as observed in the plot for a 20×20 lattice. As the lattice size increases, symmetry-based dependence is favoured and transitions become sharper. This is reflected in the plot, with steeper gradients in the magnetisation plot when moving from a 20×20 to a 60×60 lattice.

In general, heat capacity per spin tends to decrease when increasing the lattice site. This makes sense, as a material's total heat capacity stays the same regardless of lattice size. Therefore, the maximum heat capacity per spin decreases when the number of lattices (and therefore spins) is increased. A similar, but less extreme trend is observed for the magnetic susceptibility. Here, as the temperature approaches T_c , the correlation length increases, making the system more sensitive to fluctuations in spin alignment and increases the magnetic susceptibility. As $T \rightarrow T_c$, the magnetic susceptibility peak grows and shifts closer to T_c with increasing L .

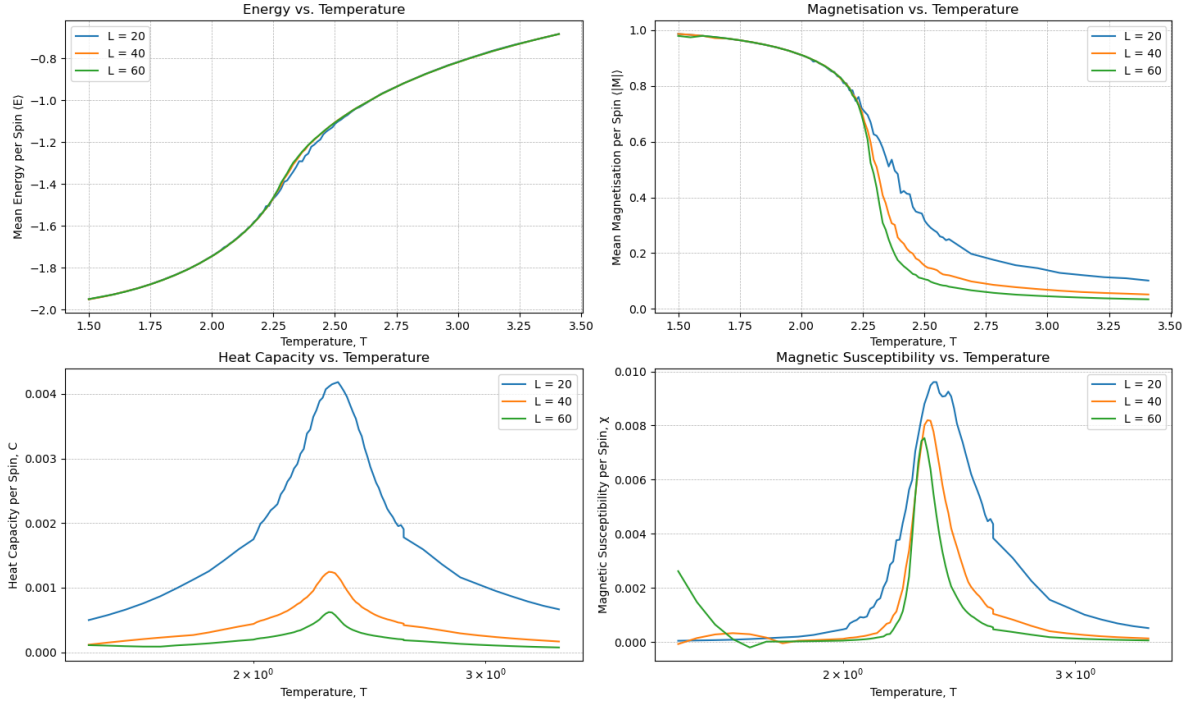


Figure 6: Plot of different observables vs. temperature for various lattice sizes

At the same time, the functions were analysed by their maximum, steepest gradient and curvature to estimate the transition temperature at zero field. The table with estimations can be found in Table 3

	T_c for $L = 20$	T_c for $L = 40$	T_c for $L = 60$
Max $\chi(T)$	2.34286	2.30612	1.55000
Max $d\chi/dT$	2.60000	2.60000	2.60000
Max $d^2\chi/dT^2$	2.58776	2.58776	2.58776
Max $C(T)$	2.31837	2.29388	2.28163
Max dC/dT	2.60000	2.60000	2.60000
Max d^2C/dT^2	2.58776	2.58776	2.58776

Table 3: Table of transition temperature estimations by various methods based on magnetic susceptibility and heat capacity

From the table, it seems as though the transition temperature at zero field is best estimated from the heat capacity plot using the maximum heat capacity values. At 2.32, 2.29 and 2.28 respectively, these are decent estimations when compared to the exact value of 2.27. Moreover, it confirms the idea that larger lattice sizes are less susceptible to changes in spin and therefore provide more accurate results. The estimated transition temperature at zero field for a 60×60 lattice is, at 2.282, only 0.6% larger than the exact value.

In summary, finite-size effects play a crucial role across all observables. The sharpness of the magnetisation drop, the peak in heat capacity and the shift in magnetic susceptibility all become more pronounced with increasing lattice size. This is consistent with the theoretical model of the 2D Ising model as described above. The behaviour observed in larger lattices approximates the limit on which the theoretical 2D Ising model is based more closely, allowing for better estimates of the transition temperature. Moreover, the smoothed plots confirm that thermal fluctuations dominate small systems but their influence diminishes as the system size increases.